

Non-linear thermal convection in a tilting porous layer

by

Enok Palm and Morten Tveitereid

Department of Mechanics

University of Oslo

ABSTRACT

This paper is concerned with thermal convection in a tilted porous layer. The basic temperature distribution is spatially non-constant, due to internal heat sources or time-dependent boundary conditions. It is shown that for small angles of inclination both hexagons and two-dimensional rolls are stable solutions. For larger angles only rolls may occur. The problem has a bearing on convection in the interior of the earth and the occurrence of "patterned ground".

Nomenclature

A_n ,	defined by (3.21);	a ,	wave number
B_q ,	defined by (3.12);	a_c ,	critical wave number;
C_n ,	defined by (3.8);	$f(z)$,	defined by (3.12);
C ,	$= (C_p)_m / (C_p)_f$;	$g(z)$,	defined by (3.13);
$(C_p)_m$,	heat capacity at constant pressure for the solid-fluid mixture;	\vec{g} ,	$= (\sin\gamma, 0, -\cos\gamma)g$, acceleration of gravity;
$(C_p)_f$,	heat capacity at constant pressure for the fluid;	h ,	depth of the layer;
∇ ,	$= (\frac{\partial}{\partial x}, \frac{\partial}{\partial y}, \frac{\partial}{\partial z})$;	$\vec{i}, \vec{j}, \vec{k}$,	unit vectors;
∇^2 ,	$= \nabla \cdot \nabla$;	\vec{k}_n	$= (k_n^x, k_n^y, 0)$, wave number vector;
∇_1^2 ,	$= \frac{\partial^2}{\partial x^2} + \frac{\partial^2}{\partial y^2}$;	k ,	permeability;
ΔR ,	$= R - (1 + \frac{1}{2}\gamma^2)R_0^{(0)}$;	p ,	pressure;
ΔT ,	temperature difference between the boundaries;	p_s ,	static pressure;
R ,	Rayleigh number;	$p_m^{(n)}$,	defined by (3.2);
R_c ,	critical Rayleigh number;	\vec{r} ,	$= (x, y, 0)$;
$R_m^{(n)}$,	defined by (3.1);	t ,	time;
R_N ,	defined by (4.1);	\vec{v} ,	$= (u, v, w)$ velocity;
T ,	temperature;	$\vec{v}_m^{(n)}$,	defined by (3.2);
T_0 ,	standard temperature;	x, y, z ,	cartesian coordinates.
$U(z)$,	defined by (2.6);		
U_0 ,	defined by (2.16);		
A, E, P, Q, S, U, V, W ,	coefficients of the amplitude equation, defined by (A.10)-(A.14);		

Greek letters

α ,	coefficient of expansion;	μ ,	viscosity;
γ ,	inclination angle (radians);	ρ ,	density;
$\vec{\delta} =$	$(\frac{\partial^2}{\partial x \partial z}, \frac{\partial^2}{\partial y \partial z}, -v_1^2)$;	ρ_0 ,	standard density;
ϵ ,	expansion parameter due to the amplitude;	σ ,	growth rate;
θ ,	temperature;	$\tau_m^{(n)}$,	defined by (3.3);
$\theta_m^{(n)}$,	defined by (3.1);	φ_N ,	defined by (4.1);
κ ,	thermal diffusivity;	ψ ,	defined by (3.10);
λ ,	inclination angle (degrees);	ω_N ,	defined by (4.1);
		$\omega = -\omega_2$.	

Superscripts

- ' , perturbation quantities;
- ^ , adjoint quantities;
- * , complex conjugate quantities.

Non-linear thermal convection in a tilting porous layer

1. Introduction

This paper is concerned with thermal convection in a tilting layer. Our interest in this problem stems partly from the rather puzzling geophysical phenomenon called patterned ground (for an authoritative review, see Washburn [1]). In subpolar regions with permafrost, or in mountain areas, the ground some places shows a rather remarkable regular pattern. Often the pattern is composed of regular polygons, close to hexagons. The polygons may be either "sorted" or "non-sorted". In the former case the borders of the polygons are stones surrounding finer materials ("stone polygons"). At sloping grounds, the polygons are usually replaced by stripes oriented down the slope. For smaller angles of inclination polygons may, however, still be observed. For larger angles the stripes prevail completely. The lateral dimensions of the polygons and stripes vary over a wide spectrum, from 20-30 cm and up to several meters.

It seems to be no satisfactory explanation for the genesis of the polygons and stripes. There has been many attempts, and parts of the phenomenon may be understood. No accepted theory exists, however, which is capable of explaining the striking regularity of the pattern which takes place under favourable conditions. Such a regular pattern has, to our knowledge, only been found in connection with thermal convection. In this case it is well known from experiments, as well as theory, that under certain conditions a regular system of stable hexagons may occur. Under other conditions a regular system of two-dimensional rolls (stripes) may exist. It is therefore natural to try to combine the occurrence of regular poly-

gons and stripes with thermal convection, or a convection of similar nature.

The idea to relate patterned ground to thermal convection is not new. It was first forwarded by Nordenskjöld [2, 3] and later recalled by Low [4]. It has also been advocated by Gripp [5], Simon and Gripp [6] and Wasintynski [7]. The two latter papers suggest that the convection is not of thermal origin, the convective medium being a kind of mud which partly is dried out at the surface by evaporation and water supply is brought in at the bottom by melting of ice. The mud is supposed to be heaviest where the water content is smallest. The configuration is therefore unstable, and a motion close to what is known from thermal convection will be set up.

The significance of convection in the genesis of patterned ground seems not to have been generally accepted by geologists. The phenomenon shows, however, several striking features which speak in favour of convection. Besides the regularity of the pattern, observations show that the hexagons are up-hexagons, i.e. upwards motion in the middle of the cells. As will be shown in section 5, this is in agreement with the assumption of convection. Moreover, also the occurrence of stripes at sloping grounds is in conformity with the existence of convection. We further mention that a rough estimate reveals that in actual cases thermal convection may well occur, though the convection will be rather slow. It may therefore be worth while to examine the hypothesis more closely. We want, however, to point out that the occurrence of convection can by no means explain the entire problem which is, indeed, very complex. Obviously freezing processes are important for the transport of stones and other materials. The role of convection is probably limited to be

responsible for the selection of the observed pattern.

When convection in earlier works was suggested to be the reason for the formation of polygons, this was done on the basis of the classical experiments by Bénard. This is a rather doubtful basis, since, as we know now, Bénard's hexagons were due to surface tension effects. In fact, gravity driven convection will, also in horizontal layers, usually have a pattern composed of two-dimensional rolls (Schlüter, Lortz and Busse [8]). To obtain hexagons some material coefficients, such as the viscosity, must be a function of the temperature, or the temperature gradient must be a function of z (for a review, see Palm [9]). In this paper we consider the last possibility, the temperature gradient being dependent on z , due to temperature variations at the boundaries.

The convection may take place in a kind of mud, or, in other cases, in a porous media. In the first example the matrix takes completely part in the convection, whereas in the second case the matrix is fixed. Most likely a combination of these extremes take place in nature.

The intention of this paper is rather limited, compared to the general problem. We shall focus our interest on the problem of thermal convection in a sloping layer, and examine the conditions for occurrence of stripes and polygons. This may throw some light on the genesis of patterned grounds. The problem has, however, also its own value. For simplicity, the layer is assumed to be porous. The results obtained are also qualitatively valid for convection in other fluids. It is necessary to apply non-linear theory and find possible solutions of the equations. To examine which solutions may be realized, we also have to apply stability analysis. We shall

find that for small angles of inclination both hexagons and stripes may exist, depending on the Rayleigh number. For larger angles hexagons become instable. Strictly speaking, the cells which here are called hexagons, are slightly deformed and, as we shall see, they move downhill with a given small velocity.

It may be pointed out that the actual problem also may be interpreted as convection set up in a tilting layer due to internal heating. This problem is of interest in the study of the interior of the earth.

2. The model

We consider a tilting porous layer of infinite lateral extent. The depth of the layer is denoted by h , the angle of inclination by γ and the x - and z -axis are placed as shown in Fig. 1. It was mentioned in the introduction that we shall consider a basic temperature gradient being z -dependent. The non-constant temperature gradient may be caused by internal heat sources or by temperature variations at the boundaries. In the last case the temperature profile is, strictly speaking, a function of time explicitly. We shall, however, disregard this explicit time dependence ("freeze" the temperature) and restrict our solution to cases where the changes of the temperature profile with time is rather moderate. In the case of internal heat sources the equations are correct without any such assumptions.

It is reasonable to assume that the lower boundary is kept at a constant temperature, such that the curvature of the temperature profile is due to temperature variations at the upper boundary. To obtain thermal convection the fluid must be unstably stratified with heavier fluid above lighter. We are therefore led to consider a temperature profile of the type shown in Fig. 1 which is obtained by cooling of the surface. However, if the lower boundary is kept at 0°C (permafrost), the temperature must increase upwards since α (the coefficient of expansion) for water then is negative. This example is also incorporated in our model if in Fig. 1 the curve displays the variation of αT rather than T .

Applying the Boussinesq approximation, the governing equations may be written

$$-\nabla p + \rho \vec{g} - \frac{\mu}{k} \vec{v} = 0 \quad (2.1)$$

$$C \frac{\partial T}{\partial t} + \vec{v} \cdot \nabla T = \kappa \nabla^2 T \quad (2.2)$$

$$\nabla \cdot \vec{v} = 0 \quad (2.3)$$

$$\rho = \rho_0 (1 - \alpha(T - T_0)) \quad (2.4)$$

Here (2.1) expresses the balances of forces in a porous medium, (2.2) is the heat equation, (2.3) the continuity equation and (2.4) the equation of state. Moreover, p denotes the pressure, ρ the density, \vec{g} the acceleration of gravity, μ the viscosity, k the permeability, $\vec{v} = (u, v, w)$ the velocity, T the temperature, t the time, κ the thermal diffusivity for the porous medium, ρ_0 and T_0 standard density and temperature, respectively, α the coefficient of expansion and C is a constant.

The upper and lower boundary are assumed to be kept at constant temperature. The boundary conditions may then be written

$$\begin{aligned} w = 0, \quad T = 0 & \quad z = -h \\ w = 0, \quad T = -\Delta T & \quad z = 0 \end{aligned} \quad (2.5)$$

where we have chosen $T = 0$ at $z = -h$. ΔT denotes the constant temperature difference over the layer.

When ΔT is small, the heat transfer is in the form of conduction. Let the temperature then be denoted by $T(z)$. The gravity will set up a velocity down the slope, $U(z)$. Assuming that $\partial p / \partial x = 0$, we find from (2.1) and (2.4) that

$$\frac{\mu}{k} U(z) = \rho_0 (1 - \alpha(T(z) - T_0)) g \sin \gamma \quad (2.6)$$

For larger ΔT , in the convective regime, we write

$$\begin{aligned}\vec{v} &= U(z)\vec{i} + \vec{v}' \\ T &= T(z) + \theta' \\ p &= p_s + p'\end{aligned}\tag{2.7}$$

where p_s is the static pressure defined by

$$-\frac{\partial p_s}{\partial z} + \rho_0(1 - \alpha(T(z) - T_0))g \cos \gamma = 0\tag{2.8}$$

Introducing (2.7) in (2.1 - 2.4), applying (2.6) and (2.8), and neglecting the dashes, gives

$$\nabla p + \rho_0 \alpha \theta \vec{g} + \frac{\mu}{k} \vec{v} = 0\tag{2.9}$$

$$\nabla \cdot \vec{v} = 0\tag{2.10}$$

$$C \frac{\partial \theta}{\partial t} + w \frac{\partial T(z)}{\partial z} + U(z) \frac{\partial \theta}{\partial x} + \vec{v} \cdot \nabla \theta = \kappa \nabla^2 \theta\tag{2.11}$$

The equations may be written in a non-dimensional form by choosing h as characteristic scale for length, κ/h for velocity, Ch^2/κ for time, $\mu\kappa/k$ for pressure, $\Delta T/R$ for θ and ΔT for $T(z)$. Here R is the Rayleigh number defined by

$$R = \frac{g\alpha\Delta T h k}{\kappa \mu / \rho}\tag{2.12}$$

Equations (2.9 - 2.11) then take the non-dimensional form

$$\nabla p + \theta(\sin\gamma\vec{i} - \cos\gamma\vec{k}) + \vec{v} = 0\tag{2.13}$$

$$\nabla \cdot \vec{v} = 0\tag{2.14}$$

$$\begin{aligned}\nabla^2 \theta - R w \frac{\partial T(z)}{\partial z} &= R(T_0 - T(z)) \frac{\partial \theta}{\partial x} \sin \gamma \\ &+ U_0 \frac{\partial \theta}{\partial x} \sin \gamma + \vec{v} \cdot \nabla \theta + \frac{\partial \theta}{\partial t}\end{aligned}\tag{2.15}$$

where

$$U_0 = \frac{g\rho_0 kh}{\kappa\mu} \quad (2.16)$$

and \vec{i} and \vec{k} denote the unit vectors in the x- and z-direction, respectively. The boundary conditions become

$$\theta = w = 0 \quad z = -1, 0 \quad (2.17)$$

3. The amplitude equations

To obtain the solution of (2.13) - (2.15) for small, but finite amplitudes we develop R and p, θ, \vec{v} in power series in the two small parameters ϵ and γ . ϵ is a measure for the amplitude in the steady state, the exact definition of ϵ is not needed. We write

$$R = \sum_{\substack{n=0 \\ m=0}} \gamma^m \epsilon^n R_m^{(n)} \quad (3.1)$$

$$(p, \theta, \vec{v}) = \sum_{\substack{n=1 \\ m=0}} \epsilon^n \gamma^m (p, \theta, \vec{v})_m^{(n)} \quad (3.2)$$

It is appropriate to introduce multiple time scales, i.e. consider (p, θ, \vec{v}) as functions of $t, \gamma t, \epsilon t, \dots$. We write

$$\tau_m^{(n)} = \epsilon^n \gamma^m t \quad (3.3)$$

whereby

$$\frac{d}{dt} = \sum_{\substack{n=0 \\ m=0}} \epsilon^n \gamma^m \frac{\partial}{\partial \tau_m^{(n)}} \quad (3.4)$$

Due to the symmetry of the problem, R must be an even function of γ . Therefore in (3.1) $R_m^{(n)} = 0$ when m uneven. Introducing (3.1), (3.2) and (3.4) in (2.13) - (2.15) and equating terms of equal power in ϵ and γ , an infinite set of linear equations result. The first of these equations became

$$\begin{aligned} \nabla_p^{(1)} - \theta_o^{(1)} \vec{k} + \vec{v}_o^{(1)} &= 0 \\ \nabla^2 \theta_o^{(1)} - R_o^{(0)} \frac{\partial T}{\partial z} w_o^{(1)} &= \frac{\partial \theta_o^{(1)}}{\partial \tau_o^{(0)}} \\ \nabla \cdot \vec{v}_o^{(1)} &= 0 \end{aligned} \quad (3.5)$$

with the boundary conditions

$$\theta_0^{(1)} = w_0^{(1)} = 0 \quad z = -1, 0 \quad (3.6)$$

These are the linearized equations for convection in a horizontal porous slab with a temperature gradient varying with z . It is rather straight forward to show that the right hand side in (3.5) is zero, i.e. the principle of exchange of stability is valid. (3.5) is an eigenvalue problem with $R_0^{(0)}$ as the eigenvalue. Let us consider solutions of (3.5) which are Fourier modes in the x, y -coordinates, i.e. solutions of the form $f(z)\exp(i\vec{k}_n \cdot \vec{r})$ where \vec{k}_n is the wave number vector and \vec{r} is the vector (x, y) . Moreover, let

$$|\vec{k}_n|^2 = a^2 \quad (3.7)$$

For a given a , there is an infinite number of wave numbers satisfying (3.7), corresponding to Fourier modes in all directions in the x, y -plane. Such a solution may be written

$$\theta_0^{(1)} = \sum_{\substack{n=-\infty \\ n \neq 0}}^{\infty} f(z)c_n(t)e^{i\vec{k}_n \cdot \vec{r}} \quad (3.8)$$

implied that \vec{k}_n fulfil (3.7). To secure that $\theta_0^{(1)}$ is real, we must have

$$c_{-n} = c_n^*, \quad \vec{k}_{-n} = -\vec{k}_n \quad (3.9)$$

The star denotes the complex conjugate, and $f(z)$ is real and independent of n . $c_n(t)$ is an unspecified amplitude to be determined by higher order terms. The eigenvalue $R_0^{(0)}$ is a function of a , and possesses a minimum value, R_c , for $a = a_c$, say.

It follows from (3.5) that the vertical component of the vorticity

city is zero. Since the velocity field is solenoidal, $\vec{v}_0^{(1)}$ is determined by a single scalarfunction ψ , and we may write

$$\vec{v}_0^{(1)} = \left(\frac{\partial^2}{\partial x \partial z}, \frac{\partial^2}{\partial y \partial z}, -\nabla_1^2 \right) \psi \equiv \vec{\delta} \psi \quad (3.10)$$

with ∇_1^2 denoting the two-dimensional Laplacian. Corresponding to (3.8), ψ may be written

$$\psi = \sum_{\substack{n=-\infty \\ n \neq 0}} g(z) c_n(t) e^{i \vec{k}_n \cdot \vec{r}} \quad (3.11)$$

$f(z)$ and $g(z)$ are found from (3.5). According to (3.6) it is appropriate to write $f(z)$ in the form

$$f(z) = \sum_{q=1} B_q \sin q \pi z \quad (3.12)$$

Here B_1 is chosen as unity. The other B_q is then determined by (3.5). $g(z)$ is found to be

$$g(z) = \sum_{q=1} \frac{B_q}{(q\pi)^2 + a^2} \sin q \pi z \quad (3.13)$$

Since (3.5) is not self-adjoint, we also need to solve the adjoint problem of (3.5) and (3.6), which are found to be

$$\begin{aligned} \nabla \hat{p} - R_0^{(o)} \frac{\partial \hat{T}}{\partial z} \hat{\theta} \vec{k} + \vec{\nabla} \hat{v} &= 0 \\ \nabla^2 \hat{\theta} - \hat{w} &= 0 \\ \nabla \cdot \vec{\hat{v}} &= 0 \end{aligned} \quad (3.14)$$

with the boundary conditions

$$\hat{\theta} = \hat{w} = 0 \quad z = -1, 0 \quad (3.15)$$

One solution of (3.14) is

$$\begin{aligned} \hat{\theta}_N &= a^2 g(z) e^{-i \vec{k}_N \cdot \vec{r}} \\ \vec{\hat{v}}_N &= \vec{\delta} \hat{\psi} ; \quad \hat{\psi} = -f(z) e^{-i \vec{k}_N \cdot \vec{r}} \end{aligned} \quad (3.16)$$

Collecting terms of order $\epsilon\gamma$, we obtain

$$\begin{aligned} \nabla_p^{(1)} - \theta_1^{(1)} \vec{k} + \vec{v}_1^{(1)} &= -\theta_0^{(1)} \vec{i} \\ \nabla^2 \theta_1^{(1)} - R_0^{(0)} \frac{\partial T}{\partial z} w_1^{(1)} &= R_0^{(0)} (T_0 - T) \frac{\partial \theta_0^{(1)}}{\partial x} \\ &+ U_0 \frac{\partial \theta_0^{(1)}}{\partial x} + \frac{\partial \theta_0^{(1)}}{\partial \tau_1^{(0)}} \end{aligned} \quad (3.17)$$

To secure that these equations have a solution, the right hand side must be normal to any solution of the adjoint problem, i.e. to (3.16) where N is arbitrary. This solvability condition leads to

$$\begin{aligned} -\langle \hat{u}_N \theta_0^{(1)} \rangle + R_0^{(c)} \langle \hat{\theta}_N (T_0 - T) \frac{\partial \theta_0^{(1)}}{\partial x} \rangle \\ + U_0 \langle \hat{\theta}_N \frac{\partial \theta_0^{(1)}}{\partial x} \rangle + \langle \hat{\theta}_N \frac{\partial}{\partial \tau_1^{(0)}} \theta_0^{(1)} \rangle = 0 \end{aligned} \quad (3.18)$$

where brackets denote integration over the intire fluid layer. The first term is easily shown to be zero. Moreover, T_0 will now be chosen such that the second term is zero (for the temperature profile (5.13) $T_0 = -0.196$). We then end up with

$$\frac{\partial}{\partial \tau_1^{(0)}} \langle \hat{\theta}_N \theta_0^{(1)} \rangle = -i U_0 k_N^x \langle \hat{\theta}_N \theta_0^{(1)} \rangle \quad (3.19)$$

where k_N^x denotes the x -component of \vec{k}_N . Introducing for $\hat{\theta}_N$ and $\theta_0^{(1)}$, (3.19) takes the form

$$\frac{\partial}{\partial \tau_1^{(0)}} C_N(t) = -i U_0 k_N^x C_N(t) \quad (3.20)$$

Similar we may collect terms of order $\epsilon\gamma^2$, ϵ^2 and so on, and thereby obtain higher order terms. This is carried out in the appendix where we have taken into account terms up to the order $\epsilon\gamma^2$, $\epsilon^2\gamma$, ϵ^3 . The various differential equations are solved by taking

into account the respective solvability conditions. The unknown functions of z are expressed as a sum of sinus terms, as in (3.12) and (3.13). It was found that it was sufficient to take into account only 10 terms. The result was checked by applying 20 terms, without obtaining any changes in the first four figures in the coefficients in the amplitude equation (3.22)

$R_2^{(0)}$, $R_0^{(1)}$, and $R_0^{(2)}$ are obtained from the solvability conditions. Introducing these expressions in (3.1) and neglecting higher order terms, we find the time-dependent amplitude equation. It is appropriate to introduce the non-scaled amplitude A_n defined by

$$A_n = \epsilon C_n \quad (3.21)$$

After some calculation the amplitude equation is found to be

$$\begin{aligned} Q\dot{A}_N = & \{ \Delta R - i\gamma Q k_N^x U_0 - \gamma^2 k_N^{x^2} E/a^2 \} A_N \\ & + \{ A + i\gamma Q [k_N^x U - (k_{N+1}^x + k_{N-1}^x) V \\ & + (k_{N+1}^y - k_{N-1}^y) (k_{N-1}^x k_{N+1}^y - k_{N+1}^x k_{N-1}^y) W/a^2] \} A_{N+1}^* A_{N-1}^* \\ & - A_N \{ P A_N A_N^* + S (A_{N+1} A_{N+1}^* + A_{N-1} A_{N-1}^*) \} \end{aligned} \quad (3.22)$$

Here $\Delta R = R - (1 + \frac{1}{2}\gamma^2) R_0^{(0)}$ and k_N^y is the y -component of the wave number. The other quantities are defined in the appendix.

The amplitude equation (3.22) is valid to the third order in the amplitude. \vec{k}_N , \vec{k}_{N+1} and \vec{k}_{N-1} are wave number vectors rotated 120° to each other. This is the only combination of three Fourier modes giving a second order term, which is necessary to obtain a solution with a hexagonal pattern. Taking into account these three

wave modes we have secured steady solution of the form we want to examine, viz. hexagons and two-dimensional rolls.

By linearizing (3.22) it is seen that the minimum critical Rayleigh number is obtained for $k_N^x = 0$, i.e. for longitudinal rolls.

4. The steady solutions

The three modes in the steady solution of (3.22) may be written in the form

$$A_N = R_N e^{i\varphi_N}, \quad \varphi_N = \omega_N t \quad (4.1)$$

where R_N and ω_N are real quantities. Since, according to linearized theory, longitudinal rolls are the most unstable solution, one of the three modes is assumed to be directed along the y -axis. Let this mode be denoted by $N = 1$. The two other modes, which are directed $\pm 120^\circ$ to the y -axis, are denoted by $N = 2, 3$. We then have

$$k_1^x = 0, \quad k_2^x = -k_3^x = \frac{1}{2}\sqrt{3} a \quad (4.2)$$

$$k_1^y = a, \quad k_2^y = k_3^y = -\frac{1}{2}a$$

Moreover, from (3.22) it follows that

$$\omega_1 = 0, \quad \omega_2 = -\omega_3, \quad R_2 = R_3 \quad (4.3)$$

It also follows that

$$\omega_2 = -\omega = -\gamma k_2^x U_0 + \gamma k_2^x (U + V - \frac{3}{2}W) R_1 \quad (4.4)$$

$$(\Delta R - \gamma^2 \frac{k_2^x{}^2}{a^2} E) R_2 + A R_1 R_2 - (P+S) R_2^3 - S R_1^2 R_2 = 0 \quad (4.5)$$

and

$$\Delta R R_1 + A R_2^2 - P R_1^3 - 2 S R_2^2 R_1 = 0 \quad (4.6)$$

Equations (4.5) and (4.6) determine the amplitudes R_1 and R_2 . One solution of the equations is readily found. viz.

$$R_1^2 = \frac{\Delta R}{P}, \quad R_2 = R_3 = 0 \quad (4.7)$$

which shows that longitudinal rolls are a solution of the steady non-linear equations. It is noted that this is the only two-dimensional roll solution.

Assuming $R_2 \neq 0$, (4.4) and (4.5) lead to a third order equation in R_1 which may have three real solutions. When $\gamma = 0$, two of the solutions give $R_1 = R_2$ whereas the third solution leads to $R_1 \neq R_2$. For small values of γ , we find that for two of the solutions the difference between R_1 and R_2 is of the order γ^2 . The third solution is of no physical interest since it may be shown to be unstable for small γ -values. It will also turn out that one of the hexagon-solutions is always unstable.

The real solution for $\theta_0^{(1)}$, say, may then be written

$$\begin{aligned} \theta_0^{(1)} = 2f(z)[R_1 \cos ay + R_2 \cos(\frac{1}{2}\sqrt{3} ax - \frac{1}{2}ay - wt) \\ + R_2 \cos(\frac{1}{2}\sqrt{3} ax + \frac{1}{2}ay - wt)] \end{aligned} \quad (4.8)$$

or equivalently,

$$\theta_0^{(1)} = 2f(z)[R_1 \cos ay + 2R_2 \cos(\frac{1}{2}\sqrt{3} ax - wt) \cos(\frac{1}{2}ay)] \quad (4.9)$$

Since R_1 is not exactly equal to R_2 (and R_3) the solution in consideration has only approximately a hexagonal pattern, the approximation being better the smaller γ is. Moreover, it is also

noted that the quasi-hexagonal pattern is moving downstream with a speed $\omega/\frac{1}{2}\sqrt{3}a$.

In the next section we will apply a stability analysis to investigate the stability behaviour for the longitudinal rolls and the hexagons.

5. The stability of the solutions

Let δA_N denote a small variation of A_N , defined by (4.1). We then have

$$\delta A_N = \delta R_N e^{i\varphi_N} + iR_N e^{i\varphi_N} \delta\varphi_N \quad (5.1)$$

Moreover, we assume that δA_N has an exponential time dependence such that

$$\delta \dot{A}_N = \sigma \delta A_N \quad (5.2)$$

where σ is the growth rate. We then obtain from (3.22)

$$\begin{aligned} & \{-Q\sigma + \Delta R - \gamma^2 k_N^x E/a^2 - 3PR_N^2 - S(R_{N+1}^2 + R_{N-1}^2)\} \delta R_N \\ & + \{AR_{N+1} - 2SR_N R_{N-1}\} \delta R_{N-1} + \{AR_{N-1} - 2SR_N R_{N+1}\} \delta R_{N+1} \\ & + \gamma Q \{k_N^x U - (k_{N+1}^x + k_{N-1}^x) V \\ & + (k_{N-1}^x k_{N+1}^y - k_{N+1}^x k_{N-1}^y) (k_{N+1}^y - k_{N-1}^y) W/a^2\} R_{N+1} R_{N-1} (\delta\varphi_{N-1} + \delta\varphi_N + \delta\varphi_{N+1}) \\ & = 0 \end{aligned} \quad (5.3)$$

$$\begin{aligned} & \{-Q\sigma R_N - AR_{N+1} R_{N-1}\} \delta\varphi_N - AR_{N+1} R_{N-1} (\delta\varphi_{N-1} + \delta\varphi_{N+1}) \\ & - \{Q\omega_N + \gamma U_0 Q k_N^x\} \delta R_N \\ & + \gamma Q \{k_N^x U - (k_{N+1}^x + k_{N-1}^x) V \\ & + (k_{N-1}^x k_{N+1}^y - k_{N+1}^x k_{N-1}^y) (k_{N+1}^y - k_{N-1}^y) W/a^2\} (R_{N+1} \delta R_{N-1} + R_{N-1} \delta R_{N+1}) \\ & = 0 \end{aligned} \quad (5.4)$$

Longitudinal rolls

In this case R_1 is given by (4.7) and $R_2 = R_3 = 0$. σ is determined by the equations

$$\{-Q\sigma + \Delta R - 3PR_1^2\}\delta R_1 = 0 \quad (5.5)$$

$$\{-Q\sigma + \Delta R - \gamma^2 k_2^2 x^2 E/a^2 - SR_1^2\}\delta R_2 + AR_1 \delta R_3 = 0 \quad (5.6)$$

$$\{-Q\sigma + \Delta R - \gamma^2 k_2^2 x^2 E/a^2 - SR_1^2\}\delta R_3 + AR_1 \delta R_2 = 0 \quad (5.7)$$

From (5.5) we find, applying (4.7)

$$Q\sigma = -2PR_1^2 \quad (5.8)$$

which shows that these modes correspond to stable disturbances.

The other σ -values are found from the determinant of (5.6) and (5.7) being zero. This gives

$$Q\sigma = \Delta R - \gamma^2 k_2^2 x^2 E/a^2 - SR_1^2 \pm AR_1 \quad (5.9)$$

Applying (4.7) the equation takes the form

$$Q\sigma = - (S-P)\frac{\Delta R}{P} + A\left(\frac{\Delta R}{P}\right)^{\frac{1}{2}} - \gamma^2 k_2^2 x^2 E/a^2 \quad (5.10)$$

In the second term on the right hand side the plus sign has been chosen which corresponds to the most unstable mode. We notice from (5.10) that for a fixed γ^2 -value, σ becomes negative for sufficiently small values of ΔR . On the other hand, for a small, but fixed value of ΔR , σ becomes positive for sufficiently small values of γ^2 . Moreover, for sufficiently large values of ΔR , σ is always negative. We also see that for γ^2 sufficiently large, σ is negative. These results are displayed in Fig. 2 where, in order to obtain some quantitative results, we have chosen the temperature profile given in Fig. 1.

Hexagons

To examine the stability of hexagons we introduce in (5.3) and (5.4) the values for ω , R_1 and R_2 given by (4.4), (4.5) and (4.6). The six equations lead to a 6×6 -determinant which give rise to a six-order equation in σ . It may be shown that the 6×6 -determinant may in fact be reduced to a 2×2 -determinant. The corresponding second order equation in σ is

$$\{Q\sigma + A R_2^2/R_1 + 2PR_1^2\}\{Q\sigma + (P+S)R_2^2\} - 2(AR_2 - 2SR_1R_2)^2 = 0 \quad (5.11)$$

The four other roots of the six-order equation in σ correspond either to stable or neutral modes.

Equation (5.11) is easily discussed when $\gamma = 0$. It is found that a subcritical region exists, i.e. instability may start for a Rayleigh number less than the critical value determined by the linear equations. Hexagons are stable for

$$\Delta R \leq \frac{A^2(2P+S)}{(S-P)^2} \quad (5.12)$$

For larger values of ΔR , hexagons become unstable. For $\gamma \neq 0$, we must apply numerical methods to discuss (5.11). The results are most easily given in a diagram, see Fig. 2. (4.5) and (4.6) give two different hexagon solutions, one corresponding to up-hexagons and one to down-hexagons. It follows from (5.11) that only up-hexagons are stable since A is positive.

An illustrative example

To illustrate the results found in this section, we have chosen the specific temperature distribution displayed in Fig. 1. The analytic form of the temperature variation is given by

$$\begin{aligned} T &= -1 - z - \sum_{p=1}^{\infty} \frac{T_p}{p} \sin p\pi z \\ &= -1 - z - 0.467 \sin \pi z - 0.093 \sin 2\pi z - 0.013 \sin 3\pi z + \dots \end{aligned} \quad (5.13)$$

We found that $R_c = 47.3$ and $a_c = 3.555$. The other findings are shown in Fig. 2.

6. Summary and conclusion

The main results obtained in the paper are shown in Fig. 2, where the applied temperature distribution is that displayed in Fig. 1. It is noted that for small γ , a subcritical instability region exists. This is, however, very small; for $\gamma = 0$ it takes place for $47.0 < R < 47.3$ and is of no practical interest. For $\gamma > 11.8^\circ$ only longitudinal rolls are stable. For $\gamma < 11.8^\circ$ a region exists where only hexagons are stable. For $\gamma = 0$ this is true for R -values larger than 47.0 and less than 51.8 . For larger R -values both hexagons and rolls may exist, but only one of the forms at the same time. This region is for $\gamma = 0$ defined by $51.8 < R < 65.9$. For still larger values of R only longitudinal rolls may be observed.

Notice that longitudinal rolls are the dominating pattern for convection in an inclined slab. For small angles of inclination and moderate supercritical Rayleigh numbers also hexagons may occur. As pointed out above, the hexagons are not true hexagons since R_1 differs somewhat from R_2 and R_3 . The difference is of order γ^2 and is negligible for very small γ -values. For more moderate values of γ , the difference becomes, however, noticeable. The hexagons, being steady in the form, is moving downwards with a given velocity. The hexagons are up-hexagons. This is due to our assumption that the temperature at the lower boundary is kept constant. This seems for us to be a natural supposition. If, on the other

hand, the temperature at the upper boundary was kept constant whereas the temperature at the lower boundary was increased, we would have obtained down-hexagons.

Our results are also valid for convection generated by internal heat sources, a problem which is mathematically identical to the actual problem.

Bories and Combarnous [10] have performed experiments in a tilted porous layer and claim to find polygons for $\gamma < 15^\circ$ and longitudinal rolls for $\gamma > 15^\circ$. The actual temperature profile in their experiments is, however, not available so that a qualitative agreement is not possible to discuss. Due to the effect of the end walls, no propagation of the hexagonal pattern takes place in their experiments. Our theoretical result is in rather fair accordance with the observations of patterned ground, discussed in the introduction, and seems to build up under the assumption that thermal (or similar) convection is an important part of the genesis.

Appendix

By substituting (3.1) - (3.4) into (2.13) - (2.14) and collecting terms of order $\epsilon\gamma, \epsilon^2, \dots$, we derive the following sets of equations

$$O(\epsilon\gamma^2): \quad \nabla p_2^{(1)} - \theta_2^{(1)} \vec{k} + \vec{v}_2^{(1)} = -\theta_1^{(1)} \vec{i} - \frac{1}{2} \theta_0^{(1)} \vec{k} \quad (\text{A.1})$$

$$\nabla^2 \theta_2^{(1)} - R_0^{(0)} \frac{\partial T}{\partial z} w_2^{(1)} = R_2^{(0)} \frac{\partial T}{\partial z} w_0^{(1)} + R_0^{(0)} (T_0 - T) \frac{\partial \theta_1^{(1)}}{\partial x} + \frac{\partial}{\partial \tau_2^{(0)}} \theta_0^{(1)}$$

where we have applied (3.20).

Solvability condition:

$$R_2^{(0)} \langle \hat{\theta}_N \frac{\partial T}{\partial z} w_0^{(1)} \rangle + \frac{\partial}{\partial \tau_2^{(0)}} \langle \hat{\theta}_N \theta_0^{(1)} \rangle = \langle \hat{U}_N \theta_1^{(1)} \rangle + \frac{1}{2} \langle \hat{w}_N \theta_0^{(1)} \rangle - R_0^{(0)} \langle \hat{\theta}_N (T_0 - T) \frac{\partial \theta_1^{(1)}}{\partial x} \rangle \quad (\text{A.2})$$

$$O(\epsilon^2 \gamma^0): \quad \nabla_{P_0}^{(2)} - \theta_0^{(2)} \vec{k} + \vec{v}_0^{(2)} = 0 \quad (A.3)$$

$$\nabla^2 \theta_0^{(2)} - R_0^{(0)} \frac{\partial T}{\partial z} w_0^{(2)} = R_0^{(1)} \frac{\partial T}{\partial z} w_0^{(1)} + \vec{v}_0^{(1)} \cdot \nabla \theta_0^{(1)} + \frac{\partial \theta_0^{(1)}}{\partial \tau_0^{(1)}}$$

Solvability condition:

$$R_0^{(1)} \langle \hat{\theta}_N \frac{\partial T}{\partial z} w_0^{(1)} \rangle + \frac{\partial}{\partial \tau_0^{(1)}} \langle \hat{\theta}_N \theta_0^{(1)} \rangle = - \langle \hat{\theta}_N \vec{v}_0^{(1)} \cdot \nabla_0^{(1)} \rangle \quad (A.4)$$

Here it is noted that the term on the right hand side in (A.4) is a very important term in our discussion, and corresponds to the part of the second order term in the amplitude equation (3.22) being proportional to A . If this term is zero, no stable solution exists with a hexagonal pattern. The term is due to the curvature of the temperature profile and is therefore equal to zero when $\partial T/\partial z$ is constant. In the steady state (i.e. $t \rightarrow \infty$) the second order term must balance the third order term whereby it follows that the coefficient for the second order term must be small. This is obviously fulfilled for large values of time since $\partial T/\partial z$ approaches a constant value when $t \rightarrow \infty$. It turns out, however, that the coefficient is rather small also for moderate values of time, which leads to $R_0^{(1)}$ and $\partial/\partial \tau_0^{(1)}$ being small. Terms containing these quantities will therefore be cancelled in what follows.

$$O(\epsilon^2 \gamma): \quad \nabla_{P_1}^{(2)} - \theta_1^{(2)} \vec{k} + \vec{v}_1^{(2)} = - \theta_0^{(2)} \vec{i} \quad (A.5)$$

$$\nabla^2 \theta_1^{(2)} - R_0^{(0)} \frac{\partial T}{\partial z} w_1^{(2)} = R_0^{(0)} (T_0 - T) \frac{\partial \theta_0^{(2)}}{\partial x} + \vec{v}_1^{(1)} \cdot \nabla \theta_0^{(1)} + \vec{v}_0^{(1)} \cdot \nabla \theta_1^{(1)} + \frac{\partial \theta_0^{(1)}}{\partial \tau_1^{(1)}}$$

where we have applied (3.20) twice.

Solvability condition:

$$\frac{\partial}{\partial \tau_1^{(1)}} \langle \hat{\theta}_N \theta_0^{(1)} \rangle = \langle \hat{u}_N \theta_0^{(2)} \rangle - R_0^{(0)} \langle \hat{\theta}_N (T_0 - T) \frac{\partial \theta_0^{(2)}}{\partial x} \rangle \quad (A.6)$$

$$- \langle \hat{\theta}_N (\vec{v}_1^{(1)} \cdot \nabla \theta_0^{(1)} + \vec{v}_0^{(1)} \cdot \nabla \theta_1^{(1)}) \rangle$$

$$O(\epsilon^3 \gamma^0): \quad \nabla p_o^{(3)} - \theta_o^{(3)} \vec{k} + \vec{v}_o^{(3)} = 0 \quad (A.7)$$

$$\nabla^2 \theta_o^{(3)} - R_o^{(6)} \frac{\partial T}{\partial Z} w_o^{(3)} = R_o^{(2)} \frac{\partial T}{\partial Z} w_o^{(1)} + \vec{v}_o^{(2)} \cdot \nabla \theta_o^{(1)} + \vec{v}_o^{(1)} \cdot \nabla \theta_o^{(2)} + \frac{\partial \theta_o^{(1)}}{\partial \tau_o^{(2)}}$$

Solvability condition:

$$R_o^{(2)} \langle \hat{\theta}_N \frac{\partial T}{\partial Z} w_o^{(1)} \rangle + \frac{\partial}{\partial \tau_o^{(2)}} \langle \hat{\theta}_N \theta_o^{(1)} \rangle = - \langle \hat{\theta}_N (\vec{v}_o^{(2)} \cdot \nabla \theta_o^{(1)} + \vec{v}_o^{(1)} \cdot \nabla \theta_o^{(2)}) \rangle \quad (A.8)$$

Introducing $R_2^{(0)}$, $R_o^{(1)}$ and $R_o^{(2)}$ into (3.1) give

$$\begin{aligned} \frac{d}{dt} \langle \hat{\theta}_N \theta_o^{(1)} \rangle &= - (R - R_o^{(6)}) \langle \hat{\theta}_N \frac{\partial T}{\partial Z} w_o^{(1)} \rangle + \gamma \frac{\partial}{\partial \tau_1} \langle \hat{\theta}_N \theta_o^{(1)} \rangle \\ &+ \gamma^2 \frac{1}{2} \langle \hat{w}_N \theta_o^{(1)} \rangle - \gamma^2 \langle \hat{u}_N \theta_1^{(1)} \rangle - \gamma^2 R_o^{(6)} \langle \hat{\theta}_N (T_o - T) \frac{\partial \theta_1^{(1)}}{\partial x} \rangle \\ &- \epsilon \langle \hat{\theta}_N \vec{v}_o^{(1)} \cdot \nabla \theta_o^{(1)} \rangle + \epsilon \gamma \frac{\partial}{\partial \tau_1} \langle \hat{\theta}_N \theta_o^{(1)} \rangle \\ &- \epsilon^2 \langle \hat{\theta}_N (\vec{v}_o^{(2)} \cdot \nabla \theta_o^{(1)} + \vec{v}_o^{(1)} \cdot \nabla \theta_o^{(2)}) \rangle \end{aligned} \quad (A.9)$$

The constants Q, E, \dots in (3.22) are defined by the relations

$$\frac{\frac{d}{dt} \langle \hat{\theta}_N \theta_o^{(1)} \rangle}{-\langle \hat{\theta}_N \frac{\partial T}{\partial Z} w_o^{(1)} \rangle} = Q \frac{\dot{C}_N}{C_N} \quad (A.10)$$

$$\frac{\langle \hat{u}_N \theta_1^{(1)} \rangle + R_o^{(6)} \langle \hat{\theta}_N (T_o - T) \frac{\partial \theta_1^{(1)}}{\partial x} \rangle}{-\langle \hat{\theta}_N \frac{\partial T}{\partial Z} w_o^{(1)} \rangle} = E \frac{k_N^x}{a^2} \quad (A.11)$$

$$\frac{-\langle \hat{\theta}_N \vec{v}_o^{(1)} \cdot \nabla \theta_o^{(1)} \rangle}{-\langle \hat{\theta}_N \frac{\partial T}{\partial Z} w_o^{(1)} \rangle} = A \frac{C_{N+1}^* C_{N-1}^*}{C_N} \quad (A.12)$$

$$\begin{aligned} \frac{\frac{\partial}{\partial \tau_1} \langle \hat{\theta}_N \theta_o^{(1)} \rangle}{-\langle \hat{\theta}_N \frac{\partial T}{\partial Z} w_o^{(1)} \rangle} &= iQ \left\{ k_N^x U - (k_{N+1}^x + k_{N-1}^x) V + \right. \\ &\left. (k_{N+1}^y - k_{N-1}^y) (k_{N-1}^x - k_{N+1}^x - k_{N+1}^y k_{N-1}^y) W / a^2 \right\} \frac{C_{N+1}^* C_{N-1}^*}{C_N} \end{aligned} \quad (A.13)$$

$$\frac{\langle \hat{\theta}_N (\vec{v}_0^{(2)} \cdot \nabla \theta_0^{(1)} + \vec{v}_0^{(1)} \cdot \nabla \theta_0^{(2)}) \rangle}{-\langle \hat{\theta}_N \frac{\partial T}{\partial z} w_0^{(1)} \rangle} = P C_N C_N^* + S(C_{N+1} C_{N+1}^* + C_{N-1} C_{N-1}^*) \quad (\text{A.14})$$

In (A.13) we have used (A.6). At last we obtain

$$\frac{\langle \hat{w}_N \theta_0^{(1)} \rangle}{-\langle \hat{\theta}_N \frac{\partial T}{\partial z} w_0^{(1)} \rangle} = -R_0^{(0)} \quad (\text{A.15})$$

Using the expression (5.13) for the temperature profile the constants are calculated to be

$$\begin{aligned} Q &= 0.4704 & U &= 0.9941 \\ E &= 40.29 & V &= 1.048 \\ A &= 1.367 & W &= 0.9915 \\ P &= 0.3245 \\ S &= 0.6918 \end{aligned}$$

REFERENCES

1. A.L. Washburn, Periglacial processes and environments. Edvard Arnold, London (1973).
2. O. Nordenskjöld, Polarvärlden och dess grannländer. Stockholm (1907).
3. O. Nordenskjöld, Wissenschaftliche Ergebnisse der Schwedischen Südpolar-Expedition 1901-1903, Bd. I. Stockholm (1920).
4. A.R. Low, Instability of viscous fluid motion, Nature CXV, 299 (1925).
5. K. Gripp, Über Frost und Strukturboden auf Spitzbergen, Zs.d.Ges.f. Erdkunde zu Berlin, 351 (1926).
6. K. Gripp und W.G. Simon, Experimente zum Brodelbodenproblem, Centralblatt für Mineralogie B, 433 (1932).

7. J. Wasintyński, Studies in hydrodynamics and structure of stars and planets, *Astrophysica Norwegica*, 4 (1946).
8. A. Schlüter, D. Lortz and F.H. Busse, On the stability of steady finite amplitude convection, *J. Fluid Mech.* 23, 129 (1965).
9. E. Palm, Nonlinear thermal convection, *Ann. Rev. Fluid Mech.* 7, 39 (1975).
10. S.A. Bories and M.A. Combaruous, Natural convection in a sloping porous layer, *J. Fluid Mech.* 57, 63 (1973).

Figure legends

Figure 1. The temperature distribution $T(z)$ and the coordinate system.

Figure 2. The stability regions of hexagons and longitudinal rolls.

——, The stability curve for hexagons.

Stable inside, unstable outside.

----, Hexagons are the only stable mode inside this curve.

....., The marginal stability curve for two-dimensional rolls.

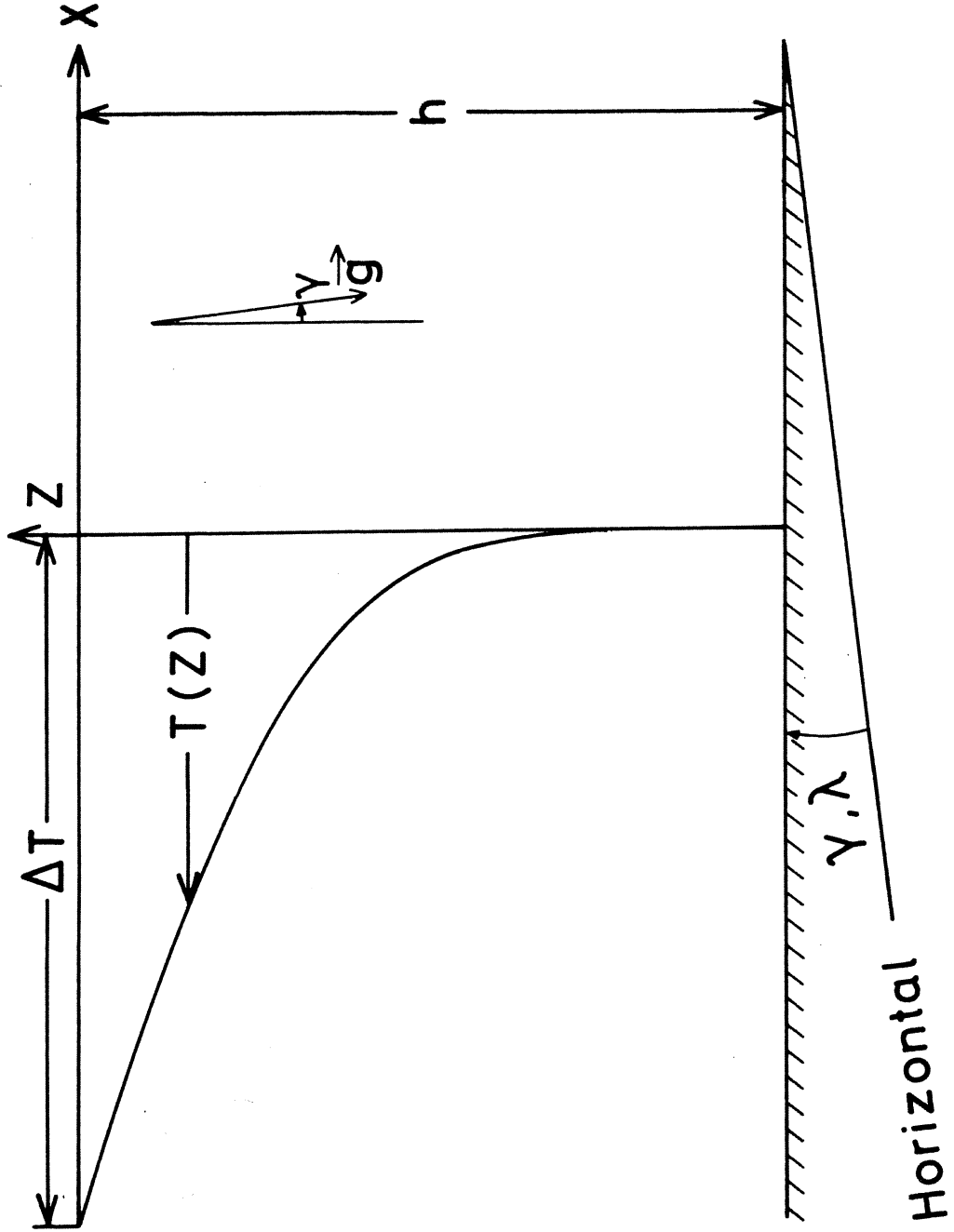


Figure 1

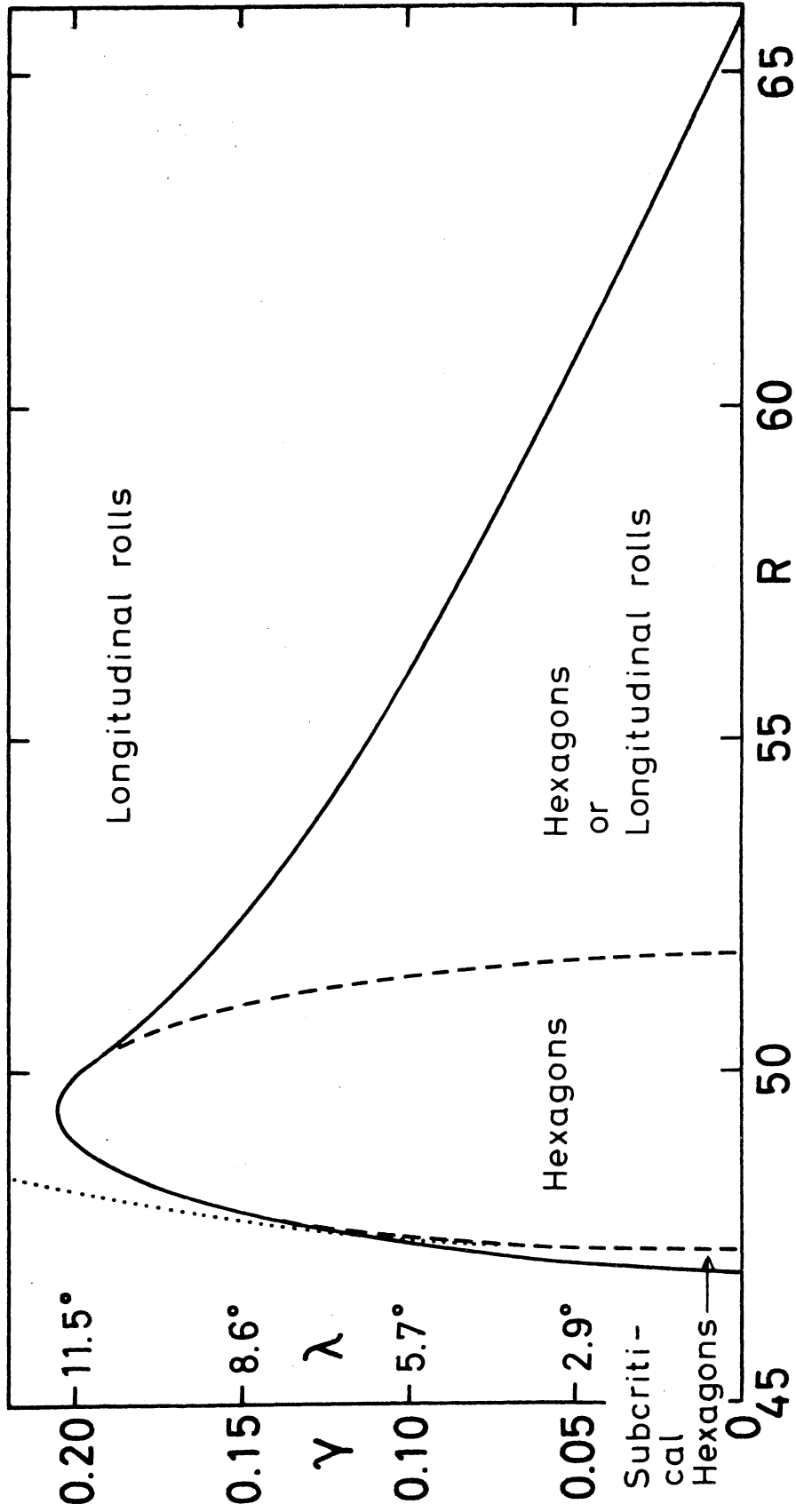


Figure 2